The Journal of Experimental Biology 211, 3421-3432
Published by The Company of Biologists 2008
doi:10.1242/jeb.020479

To bend a coralline: effect of joint morphology on flexibility and stress amplification in an articulated calcified seaweed

Patrick T. Martone* and Mark W. Denny

Hopkins Marine Station of Stanford University, Pacific Grove, CA 93950, USA

*Author for correspondence at present address: Department of Botany, University of British Columbia, Vancouver, BC, Canada, V6T 1Z4 (e-mail: pmartone@interchange.ubc.ca)

Accepted 6 September 2008

SUMMARY

Previous studies have demonstrated that fleshy seaweeds resist wave-induced drag forces in part by being flexible. Flexibility allows fronds to 'go with the flow', reconfiguring into streamlined shapes and reducing frond area projected into flow. This paradigm extends even to articulated coralline algae, which produce calcified fronds that are flexible only because they have distinct joints (genicula). The evolution of flexibility through genicula was a major event that allowed articulated coralline algae to grow elaborate erect fronds in wave-exposed habitats. Here we describe the mechanics of genicula in the articulated coralline *Calliarthron* and demonstrate how segmentation affects bending performance and amplifies bending stresses within genicula. A numerical model successfully predicted deflections of articulated fronds by assuming genicula to be assemblages of cables connecting adjacent calcified segments (intergenicula). By varying the dimensions of genicula in the model, we predicted the optimal genicular morphology that maximizes flexibility while minimizing stress amplification. Morphological dimensions of genicula most prone to bending stresses (i.e. genicula near the base of fronds) match model predictions.

Key words: adaptation, biomechanics, *Calliarthron*, decalcification, drag, flexibility, geniculum, intertidal, macroalgae, material properties, modulus.

INTRODUCTION

Researchers have long studied morphological adaptations that allow intertidal macroalgae to survive the hydrodynamic forces imposed by breaking waves (e.g. Delf, 1932; Koehl, 1986; Carrington, 1990; Dudgeon and Johnson, 1992; Friedland and Denny, 1995; Blanchette, 1997; Gaylord, 1997; Bell, 1999; Denny and Gaylord, 2002; Boller and Carrington, 2006; Harder et al., 2006). One unifying characteristic that has been thoroughly explored in these studies is flexibility. By being flexible, macroalgae 'go with the flow', limiting drag forces by reducing the thallus area projected into rapid flow, reconfiguring into more streamlined shapes, and bending over into slower moving water (Koehl, 1986; Gaylord and Denny, 1997; Denny and Gaylord, 2002; Boller and Carrington, 2006). Thus, for plants and algae growing in habitats characterized by unstable flow, flexibility is not only considered adaptive (Vogel, 1984) but is also generally regarded as a 'pre-requisite for survival' (Harder et al., 2004).

Unfortunately, because fleshy macroalgae probably evolved from fleshy (flexible) ancestors, adaptive hypotheses are difficult to test; flexibility may be a matter of default, rather than of design. In contrast, coralline algae (Corallinales, Rhodophyta) are firmly calcified and have a fossil record that extends back hundreds of millions of years (Johnson, 1961; Wray, 1977; Steneck, 1983). According to this fossil record, about 100 million years ago, coralline algae evolved articulations, called genicula, that gave flexibility to calcified fronds (Johnson, 1961; Wray, 1977; Steneck, 1983). This evolutionary innovation allowed coralline algae to grow away from the substratum and produce elaborate articulated fronds – not just encrusting thalli – in hydrodynamically stressful conditions. Thus, for coralline algae, the evolutionary transition from inflexible to flexible thalli is clear. And articulated coralline algae have been ecologically successful: they are prevalent in oceans worldwide with some species, such as the coralline *Calliarthron cheilosporioides* Manza (Fig. 1A), often dominating wave-exposed low-intertidal habitats.

Despite the ecological and mechanical success of articulated coralline algae, the mechanics of articulated fronds are poorly understood. While fleshy algae are flexible along the entire length of their thalli, the flexibility of articulated coralline algae is confined to discrete positions along otherwise rigid thalli. The effect of this distinct segmented morphology on bending performance and stress amplification is an open question.

Genicula in the articulated coralline *Calliarthron* are composed of thousands of elongated cells (Martone, 2007). The distal ends of each flexible genicular cell remain firmly calcified and embedded in adjacent intergenicula (Johansen, 1969; Johansen, 1981), thereby tethering intergenicula together. Moreover, unlike cells in most plant tissues, adjacent genicular cells are only loosely connected to one another. Genicular cells fray and separate as genicula break (P.T.M. and M.W.D., unpublished observations), possibly due to minimal and weak middle lamella between cells. These qualities suggest that a *Calliarthron* geniculum may be modeled not as a single solid but, rather, as a collection of straight cables capable of sliding past one another with minimal shear resistance.

In this study, we describe the geometry of bending genicula and introduce a computational model that utilizes genicular geometry to predict deflections of articulated fronds. By varying genicular dimensions in the model, we tested the effect of articulated frond morphology on flexibility and genicular stress amplification. We predicted optimal genicular dimensions that maximize flexibility (thereby reducing drag force) while minimizing stress (thereby reducing risk of breakage), and tested whether genicula subject to the greatest bending stresses (i.e. those nearest frond bases) adhered to our predictions.

MATERIALS AND METHODS

Genicular geometry

The morphology of *Calliarthron* genicula is illustrated in Fig. 1. Genicula have initial length ω, are separated by calcified intergenicula of length L, and are bounded laterally by intergenicular lips of length x (Fig. 1B). Fronds are generally flattened, branching in two dimensions, and genicula are elliptical in cross-section with major radius r_1 and minor radius r_2 (Fig. 1C). Because flexural stiffness is proportional to the cube of bending radius (Wainwright et al., 1982), genicula are presumed to be more flexible when bent over the shorter minor radius (i.e. around the longer major radius). We assume genicula always bend around r_1, as fronds reorient under breaking waves. Genicula are circumscribed by elliptical intergenicula with minor radius y (Fig. 1C). Genicula and intergenicula are assumed to be concentric.

Measuring tensile modulus (E_t)

Determining the stiffness or tensile modulus (E_t) of genicular tissue was central to modeling the mechanics of genicular bending. Fifteen *Calliarthron* fronds were collected from the low-intertidal zone in a moderately wave-exposed surge channel at Hopkins Marine Station in Pacific Grove, CA, USA. The field site was identical to that described previously (Martone, 2006; Martone, 2007). In each trial (N=15), a frond was secured between the grips of a custom-made tensometer (see Martone, 2006), allowing several intergenicula and genicula to 'float' between the grips. Paper tabs were glued to the two intergenicula flanking a single unflawed geniculum near the base of each experimental frond. The tensometer pulled fronds apart at 1 mm s^{-1}, while a video dimension analyzer (model V94, Living Systems Instrumentation, Burlington, VT, USA) measured the distance between the paper tabs under a dissecting microscope. In this manner, applied force (±0.002 N) and change in genicular length (±0.6 μm) were measured concurrently. Extension was continued until fronds broke. Stretched genicula were freshly cross-sectioned with a razor blade, and initial cross-sectional areas were calculated by measuring the inner diameters (±27 μm) of the circumscribing calcified tissue, which is unaffected by genicular deformation, using an ocular dial-micrometer. One geniculum neighboring each experimental geniculum was long-sectioned and its length (±27 μm) was measured using the ocular dial-micrometer. Standard deviation of genicular length was low (<7% of the mean), and stretched genicula were assumed to be identical in length to neighboring genicula. Nominal stress (force/unstretched cross-sectional area) *versus* engineer's strain (change in length/initial length) was plotted for one experimental geniculum in each frond. Tensile moduli (E_t) were calculated as the slopes of linear stress–strain regressions forced through the origin. Mean E_t (N=15) was used in the bending model described below.

Bending model

Deflections of articulated fronds were modeled numerically. Complete details of the bending model are included in Appendix A. In brief, breaking waves apply drag force, F, in the direction of flow, parallel to the substratum and perpendicular to initial frond orientation. At each geniculum, drag generates external bending moments that are resisted by internal moments within genicular tissue. By setting external and internal moments equal to one another, we calculated angles, ϕ, to which genicula must bend to attain equilibrium and, thereby, estimated frond deflections. This study focused on the basal-most 10 genicula – where bending was expected to be greatest – and drag was simplified to be a downstream force applied to the end of the tenth intergeniculum (Fig. 2).

Testing the bending model

Ten *Calliarthron* fronds were collected from the field site described above. Branches were removed from each frond by cutting below the first dichotomy, and the remaining straight chains of segments (generally the first 10–20 genicula) were tested as follows. For each trial, fronds were gripped by the first few genicula in clamps and held horizontal; consequently, the first three to five genicula in each test frond were hidden within the clamps and were not tested here. A thread lasso was tied and glued around the eleventh geniculum

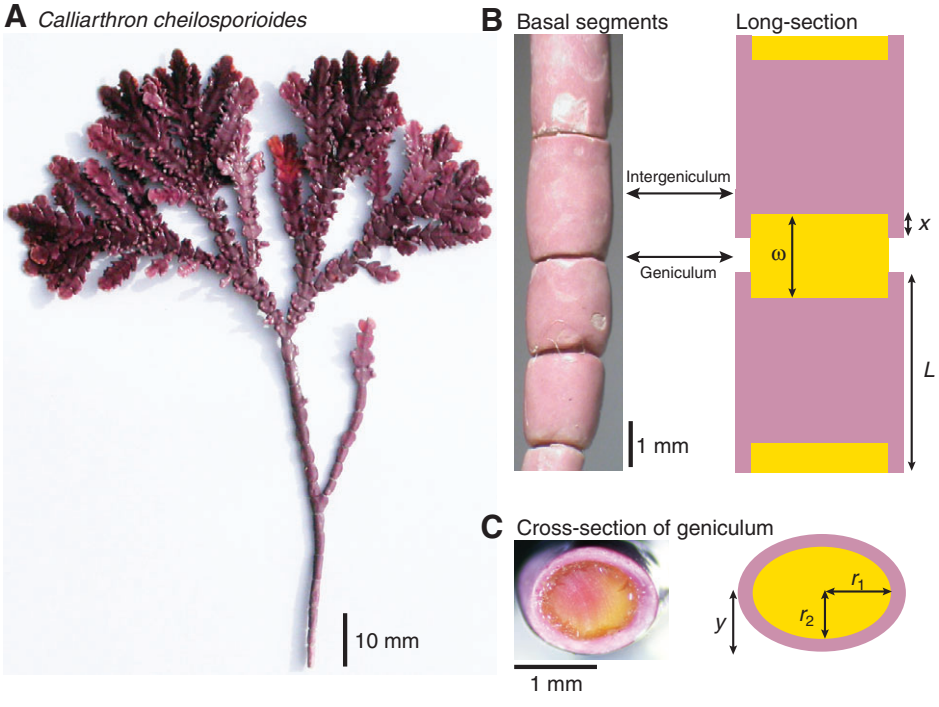

Fig. 1. (A) The articulated coralline *Calliarthron cheilosporioides*, including (B) long-section and (C) cross-section diagrams of genicula (yellow) and intergenicula (pink). Dimensions are genicular length ω, intergenicular length L, intergenicular lip length x, intergenicular radius y and genicular radii r_1 and r_2. Genicula are shown in yellow; intergenicula are shown in pink.

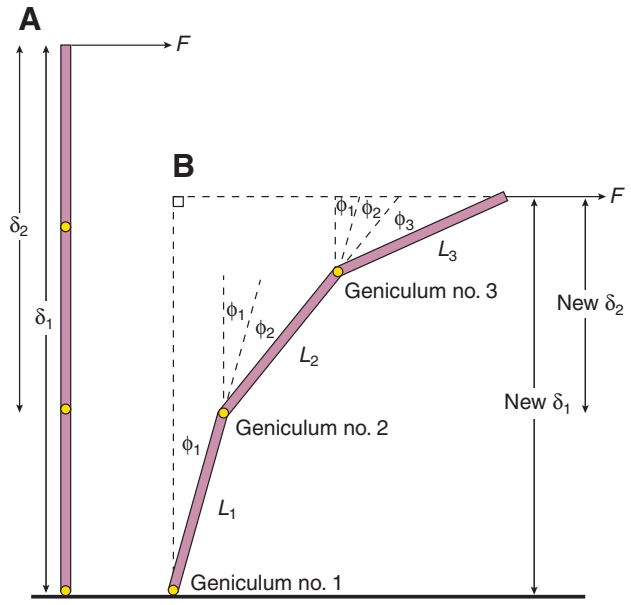

Fig. 2. Deflection of an articulated frond given an applied force, *F*, indicating (A) initial and (B) final positions. For clarity, only three segments are illustrated here. Moment arm δ_i, bending angle ϕ_i and length of distal intergeniculum L_i are indexed for each geniculum no. *i*, numbered from the base (see Appendix A for details).

from the clamp (just distal to the tenth intergeniculum), from which 5, 20 and 100 g masses were hung. Forces applied by these masses (0.05, 0.20 and 0.98 N) generated a wide range of frond deflections and corresponded to drag forces experienced by large fronds (planform area, 30 cm^2) in intertidal water velocities of 0.5, 1.6 and 4.4 $m\,s^{-1}$, respectively [see equations 4 and 12 in the accompanying paper (Martone and Denny, 2008)]. These are typical (if not conservative estimates) of water velocities characterizing wave-exposed rocky intertidal habitats (Bell and Denny, 1994; Denny, 1995; Denny et al., 2003; O'Donnell, 2005). Digital photos were taken of each deflection immediately after load application, and genicular positions were obtained using an image analysis routine (ImageJ, NIH Image, http://rsb.info.nih.gov/ij/).

After each trial, genicular dimensions were measured for all 10 genicula bent in each frond. First, intergenicular lengths (L) and unstressed gaps between intergenicula (ω–$2x$) were measured using the ocular dial-micrometer. Genicula were then freshly cross-sectioned with a razor blade and intergenicular radii (y) and genicular radii (r_1, r_2) were measured directly. Because cross-sectioned genicula could not also be long-sectioned, the lengths (ω) of two to three genicula outside the chain of 10 segments were measured after being decalcified and long-sectioned. Standard deviations of these measurements were generally low (<10% of the mean), and mean genicular length was used for all 10 genicula. Intergenicular lip length (x) was estimated for each geniculum as half the difference between gap length and mean genicular length.

Genicular dimensions for each frond were input into the numerical model to make bending predictions. Model accuracy was analyzed qualitatively by graphing real and model deflections together and quantitatively by comparing (1) real and predicted bending angles of first genicula and (2) real and predicted deflection of whole fronds, calculated as arctan(x-coordinate/y-coordinate) of the frond tip relative to the frond base.

Estimating maximum stress

As articulated fronds bend, basal genicula experience the greatest bending moments and the greatest bending stresses. After predicting deflections of articulated fronds, the numerical model estimated the maximum stress within the first genicula of our sampled fronds based on genicular morphology and bending angles. Mathematics describing these stress calculations are provided in Appendix B.

Effect of genicular characteristics on stress and flexibility

The computational model was used to evaluate the effects of genicular dimensions on (1) frond flexibility, inferred from the deflection angle of entire fronds, calculated as arctan (x-coordinate/y-coordinate) of the frond tip relative to the frond base, and (2) maximum stress within first (basal) genicula. Mean values for genicular dimensions were calculated from all *Calliarthron* genicula bent in the 10 trials (ω, N=27; all other dimensions, N=100) and were assumed to be constant along a virtual 'average' frond. Data for the average frond were entered in the bending model and tested at F=0.2 N. Holding all other dimensions constant at their mean values, each dimension (ω, x, E_t, y, L, r_1 and r_2) was varied independently and the resulting frond deflections were recorded. To explore the overall effect of genicular radius, r_1 and r_2 were varied concurrently and in the same proportion. When intergenicular length was varied, the number of intergenicula was adjusted to hold overall frond length constant (e.g. half as many intergenicula, twice as long as the mean). In one trial, genicular dimensions were all held constant but tensile modulus was allowed to vary. Because hypothetical values of some dimensions were limited by others (e.g. intergenicular lips could not be longer than half the length of genicula, genicular radii could not be broader than intergenicular radii), the hypothetical range of each dimension differed, so each dimension was experimentally varied in different proportions. Frond flexibility and maximum stress were quantified in each trial, and percentage change (from average) in flexibility and stress were plotted against percentage change (from average) in genicular dimensions. The ratio of percentage change in flexibility (a potential benefit) to percentage change in stress (a potential cost) was plotted against percentage change of each genicular dimension. This benefit:cost index was used to explore changes in genicular dimensions that would increase flexibility or decrease stress and thereby improve bending performance. Shifts in genicular dimensions that increased the benefit:cost index were assumed to be beneficial, while shifts that decreased the index were assumed to be detrimental. Hypothetical genicular dimensions were assumed to be 'optimal' if they were positioned at critical points along benefit:cost index curves, such that further change in that dimension, positive or negative, decreased the benefit:cost ratio.

Optimal genicular morphology

Results from the flexibility/stress analysis were used to predict dimensions of genicula optimized for bending. Genicula that experience the most bending (hereafter called 'bending' genicula; e.g. genicula no. 1 and no. 2, nearest the base) and genicula that experience little bending and mostly tension (hereafter called 'tensile' genicula; e.g. genicula no. 11 and no. 12, farther from the base) were compared in 10 *Calliarthron* fronds collected from the field site described above. Genicular and intergenicular radii were measured in cross-sections of genicula no. 1 and no. 11, and genicular length, intergenicular length and intergenicular lip length were measured in decalcified long-sections of genicula no. 2 and no. 12 as described above. Student's paired t-tests were used to compare characteristics of bending and tensile genicula.

RESULTS

Tensile modulus

Stress–strain curves were approximately linear (Fig. 3). Mean tensile modulus of genicular tissue was 27.7±6.8 MN m^{-2} (mean ± 95% confidence interval, CI).

Bending model

The bending model predicted articulated frond deflections with reasonable accuracy (Fig. 4). In general, real and predicted angles of first genicula were similar at all test forces (Table 1). At the lowest force (F=0.05 N), slight over-prediction of bending angles near the base of the fronds caused slight over-prediction of frond deflections. Error in predicting deflection angles decreased with increasing force. At the greatest applied force (F=0.98 N), the bending model predicted frond deflections within 1–2 deg. (Table 1).

Effect of genicular characteristics on stress and flexibility

Average genicular dimensions are listed in Table 2. Adjustments to genicular dimensions had varying effects on average frond deflections (Fig. 5). Increasing all genicular dimensions increased frond stiffness, except for increasing genicular length, which decreased frond stiffness (Fig. 5A). Decreasing genicular length by 25% and increasing intergenicular length by 400% made fronds the most stiff (Fig. 5A,D). Increasing tensile modulus had little effect on overall frond stiffness. For example, increasing intergenicular length and intergenicular radius by 100%, increasing genicular radii by 50%, and increasing intergenicular lip length by 25% had greater effects on frond stiffness than quadrupling tensile modulus (Fig. 5).

Adjustments to genicular dimensions had varying effects on flexibility and stress (Fig. 6). As genicular length increased and as genicular radii, intergenicular lip length and tensile modulus decreased, flexibility increased while stress cycled between decreasing and increasing trends (Fig. 6A–C,F). As intergenicular length and intergenicular radius increased, flexibility decreased while stress increased (Fig. 6D,E).

Contrasting effects of genicular dimensions on frond deflections and stress within first genicula were accounted for by plotting the benefit:cost ratio of flexibility to stress (Fig. 7). Increasing genicular length or decreasing intergenicular lip length, intergenicular length or tensile modulus had the greatest positive effects, increasing the benefit:cost ratio for small changes (~25–30%) in those dimensions (Fig. 7). Further reduction of intergenicular lip length and tensile modulus, or increase in genicular length decreased the benefit:cost ratio. Average values for genicular and intergenicular radii were approximately optimal along benefit:cost curves, such that substantially increasing or decreasing these values reduced the benefit:cost ratio.

Differences among bending and tensile genicula

Several aspects of morphology differed significantly among bending and tensile genicula (Table 3). As predicted by changes in the benefit:cost ratio, bending genicula were flanked by significantly shorter intergenicula (P<0.001; Table 3) and had significantly shorter intergenicular lips (P<0.001; Table 3) than tensile genicula. Bending genicula also tended to be longer than tensile genicula (Table 3), although the trend was not significant (P=0.08). Genicular and intergenicular radii were not significantly different among bending and tensile genicula (P>0.60 and P=0.15, respectively).

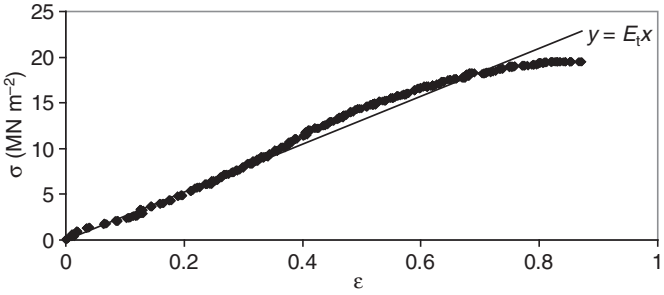

Fig. 3. Representative stress–strain (σ–ε) curve of *Calliarthron* geniculum. Tensile modulus was calculated from the slope of the linear regression.

DISCUSSION

A simple bending model

Despite their superficial simplicity, *Calliarthron* genicula are complex structures. They are composed of loosely connected cells that interact through a middle lamella of unknown composition and with unknown shear resistance. The cells produce cell walls that vary in composition and structure through time and across individual genicula (Martone, 2006; Martone, 2007). Moreover, these dynamic structures are surrounded by calcified intergenicular lips that may grind down, deform or break when genicula bend. Nevertheless, the geometric model described here estimates frond deflections with reasonable success, allowing for a detailed analysis of articulated frond performance.

Many studies have modeled the bending of biological structures using standard beam theory (e.g. Koehl, 1977; Vogel, 1984; Denny, 1988; Niklas, 1992; Etnier, 2003). For example, erect seaweeds, such as stipitate kelps, are thought to deform like cantilevered beams (Koehl, 1986; Denny, 1988; Gaylord and Denny, 1997). Our early attempts to model genicula as solid beams under-predicted frond deflections. Instead, the model presented here treats genicula not as solids but as assemblages of independent cables (genicular cells) with zero shear resistance (see details in Appendix A) – although the presence of some slight shear resistance may explain why the model initially over-predicts deflections at low strains. The similarity of real and predicted frond deflections reported here suggests that genicular cells may, indeed, behave like separate elements sliding past one another, potentially a structural adaptation for increasing flexibility.

Under breaking waves, articulated corallines bend, reorient and go with the flow. This drag-induced bending can lead to mechanical

Table 1. Error in predicting angles of first genicula and deflection of frond tips (N=10)

	Angle of first geniculum			Deflection of frond tip		
Force (N)	Mean (deg.)	Mean predicted (deg.)	Difference (deg. ± 95% CI)	Mean (deg.)	Mean predicted (deg.)	Difference (deg. ± 95% CI)
0.05	19.1	23.3	5.1±3.3	55.0	72.1	17.1±4.9
0.20	28.5	29.6	5.0±1.7	70.6	78.9	8.3±3.2
0.98	46.0	37.8	8.7±4.0	82.1	82.5	1.3±0.7

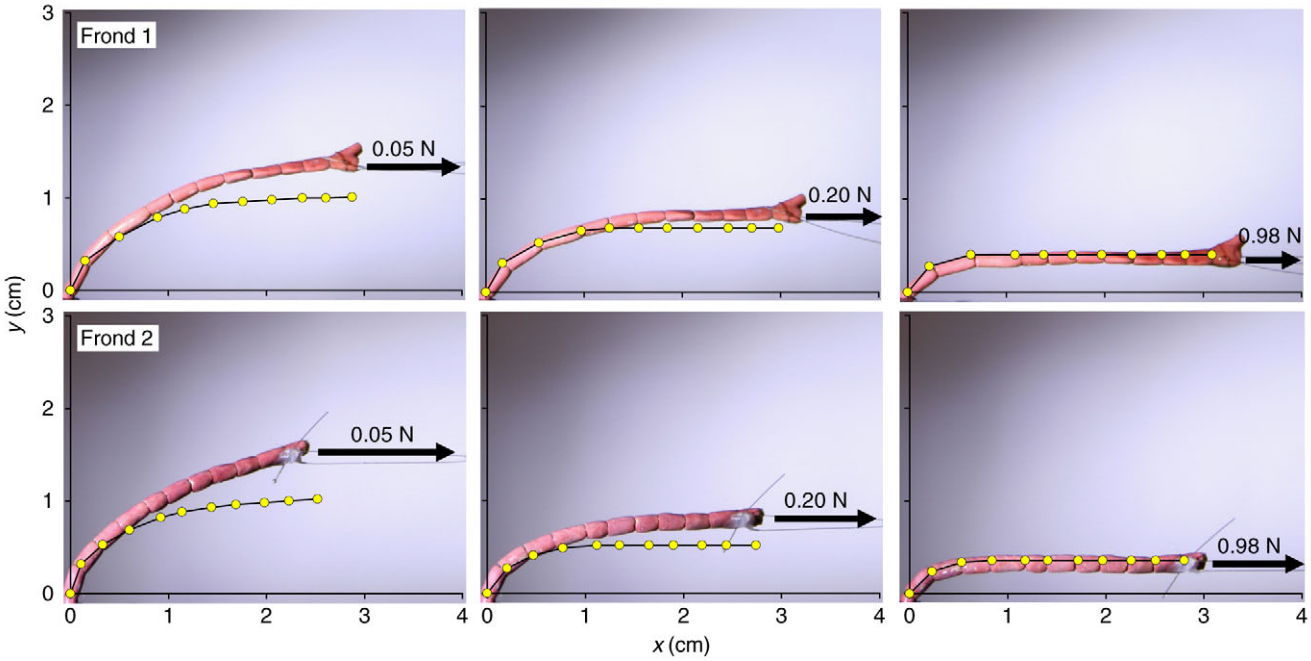

Fig. 4. Comparison of bending model predictions and observed frond deflections for two representative fronds and three applied forces.

failure, as articulated fronds are sometimes cast ashore having broken at basal genicula (Martone, 2006). Our data suggest that frond flexibility and the amplification of stress within genicula are both affected by variation in genicular dimensions. Increasing flexibility presumably benefits articulated fronds by decreasing thallus area projected into flow and by increasing reconfiguration, thereby decreasing drag, but may also increase stress. Increasing tissue stress negatively affects algae by increasing the likelihood of breakage. Adjustments to genicular dimensions that increase the ratio of flexibility to stress can be considered net benefits for articulated fronds and potential adaptations to drag-induced bending. These adjustments are described below.

Morphological adaptations to bending articulated fronds

Long genicula

According to the computational model, lengthening genicula makes fronds more flexible and, up to a point, reduces tissue stress – two qualities that benefit articulated fronds. Thus, it is reasonable to hypothesize that long genicula are adaptations to bending. This hypothesis is supported by patterns of genicular development and variation in genicular length along individual fronds. *Calliarthron* genicula consist of a single tier of cells that elongate as they develop (Johansen, 1969; Johansen, 1981). Mature genicular cells are nearly 100 times longer than they are wide (see Martone, 2007) and are approximately 10 times longer than adjacent calcified cells in the intergeniculum (Johansen, 1969). Furthermore, genicula near the bases of fronds – here called 'bending' genicula because they probably experience the most bending – tend to be longer than genicula further up the frond (Table 3).

This hypothetically adaptive growth pattern may be both biologically and mechanically limited. *Calliarthron* genicular cells lose cytoplasm and organelles as they elongate and may, therefore, be developmentally incapable of growing any longer. Furthermore, data generated by our computational model suggest that, beyond some critical length, elongating genicula may increase tissue stress (Fig. 6A), limiting the selective pressure to lengthen. This non-linear trend in tissue stress reflects the subtle numerical interaction between genicular length (ω), bending angle (ϕ), and intergenicular contact angle (β; see Eqn A32 in Appendix B).

Short intergenicular lips

Similar in effect to lengthening genicula, shortening intergenicular lips makes fronds more flexible and initially reduces tissue stress (Fig. 6C). However, our data suggest that, below some critical length, reducing intergenicular lip length may increase tissue stress. Fine-tuning of intergenicular lips to minimize tissue stress may occur in reality, as intergenicular lip length changes dynamically over time. Calcified lips initially form when genicula decalcify, thereby separating adjacent intergenicula. The remaining intergenicular tissue becomes meristematic, recovering from the effects of localized decalcification, and calcified lips grow toward one another. At the same time, calcified lips abrade and grind one another down as fronds bend in the field (Johansen, 1981). Thus, the length of intergenicular lips is self-adaptive, depending upon two antagonistic processes: growth and abrasion. Morphological data support the model conclusions; intergenicular lips of bending genicula are indeed significantly reduced (Table 3), but are never completely absent.

Table 2. Mean genicular dimensions used in bending model analysis

Dimension	Mean (mm) ± 95% CI
Genicular length, ω	0.57±0.02
Major genicular radius, r_1	0.57±0.02
Minor genicular radius, r_2	0.46±0.02
Intergenicular lip length, x	0.20±0.01
Intergenicular length, L	3.31±0.16
Intergenicular radius, y	0.69±0.02

ω, N=27; all other dimensions, N=100.

Table 3. Morphological differences among bending and tensile genicula

	Bending genicula	Tensile genicula	*t*-test
Genicular length (mm)	0.59±0.04	0.55±0.04	P=0.08
Major genicular radius (mm)	0.55±0.05	0.56±0.05	n.s.
Minor genicular radius (mm)	0.48±0.04	0.49±0.08	n.s.
Intergenicular lip length (mm)	0.08±0.03	0.19±0.03	P<0.001
Intergenicular length (mm)	1.35±0.14	3.77±0.70	P<0.001
Intergenicular radius (mm)	0.67±0.07	0.70±0.07	n.s.

N=10 pairs; mean ± 95% CI; n.s., not significant.

Short intergenicula

Shortening intergenicula makes fronds more flexible by increasing the spatial density of joints along articulated fronds. The effect of joint density on stiffness has been documented for other segmented biological beams (e.g. Etnier, 2001). As a consequence of greater flexibility, shorter intergenicula reduce the lever arm of applied forces, which lowers the moment and stress in bending genicula. Thus, shortening intergenicula both minimizes stress and maximizes flexibility. This adaptive hypothesis is borne out within individual fronds: intergenicula separating bending genicula near frond bases are significantly shorter than those separating more distal tensile genicula (Table 3). Unlike intergenicular lip length, which may fluctuate with growth and abrasion, intergenicular length is likely to be under strict biological control: shorter intergenicula probably consist of fewer (or shorter) tiers of calcified cells laid down during development. Whether intergenicular length is a plastic response to wave-induced bending stresses is unknown, but subtidal *Calliarthron*, which probably experience less drag, may be able to persist with longer intergenicula, although preliminary comparisons of articulated

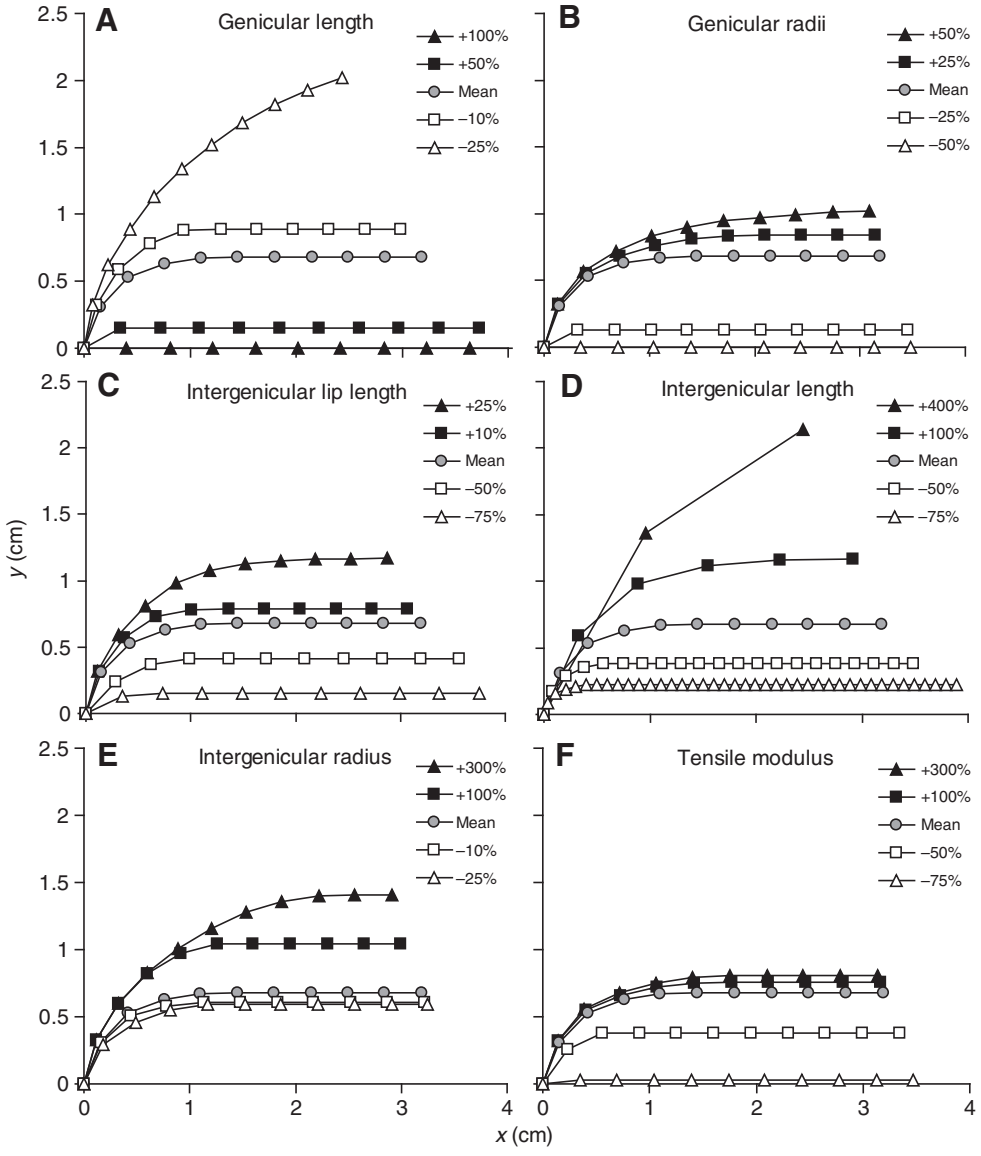

Fig. 5. Effect of varying genicular dimensions on frond deflection. (A) Genicular length, ω, (B) genicular radii r_1 and r_2, (C) intergenicular lip length x, (D) intergenicular length L, (E) intergenicular radius y and (F) tensile modulus, E_t.

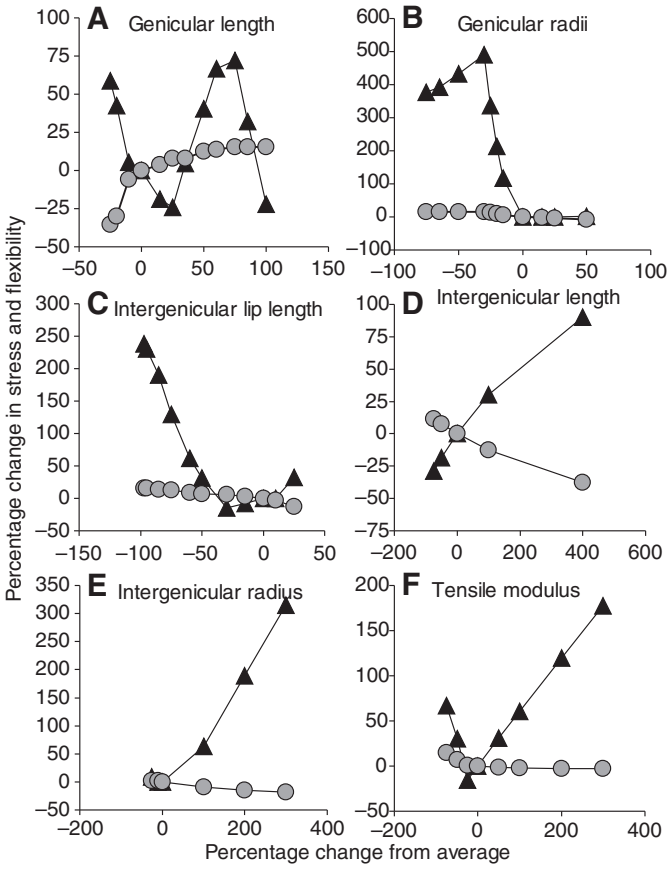

Fig. 6. Effect of varying genicular dimensions on the maximum stress within first genicula (triangles) and the deflection angle of whole fronds (circles). *x*-axes represent percentage change in (A) genicular length ω, (B) genicular radii r_1 and r_2, (C) intergenicular lip length *x*, (D) intergenicular length *L*, (E) intergenicular radius *y* and (F) tensile modulus E_t. Note that axes have differing scales.

fronds collected from different habitats suggest little site-to-site variation in intergenicular length.

Taken to its logical conclusion, this adaptive hypothesis suggests that articulated fronds should have infinitely short intergenicula to experience none of the disadvantages of segmentation. Such seaweeds would resemble fleshy macroalgae. That intergenicula are not infinitely short suggests that complete decalcification might be disadvantageous. For example, calcification minimizes the impact of herbivores on coralline fronds (Steneck, 1986; Padilla, 1993). Alternatively, there may be some metabolic cost associated with decalcification, suggesting a trade-off between energy allocation and biomechanical performance. The observed density of joints in *Calliarthron* may reflect the least number of joints sufficient to reduce stress, increase flexibility and permit survival of articulated fronds.

Unmodified genicular and intergenicular radii

According to the computational model, decreasing genicular radii and increasing intergenicular radii greatly increase tissue stress (Fig. 6B,E). Conversely, increasing genicular radii and decreasing intergenicular radii have minor effects on flexibility. As a result, substantial change in either radial dimension negatively affects articulated fronds (Fig. 7). Thus we would not expect to find adaptive shifts in genicular or intergenicular radii within bending genicula. As expected, neither radial dimension was significantly different among bending and tensile genicula (Table 3).

Interestingly, although the radii of the basal 10 genicula are generally similar, genicular radii decline measurably from base to tip within *Calliarthron* fronds (Martone, 2006). Slender, more distal, genicula are unlikely to experience much bending, but rather resist drag on distal segments in tension. Thus, reduced genicular radius is not necessarily maladaptive in these distal genicula. On the contrary, thinner genicula support fewer segments in flow and, therefore, are subject to less drag; the smallest (most apical) genicula may be over-designed for this purpose (Martone, 2006).

Decreased tensile modulus

According to the model, a slight decrease in tensile modulus would increase flexibility and reduce tissue stress (Fig. 6F). However, anything beyond a slight decrease would drastically increase stress, potentially limiting the selective pressure to reduce the tensile modulus. For example, either decreasing or increasing the tensile modulus by 50% has comparable effects on the benefit:cost ratio (Fig. 7). *Calliarthron* genicular tissue is actually quite stiff compared

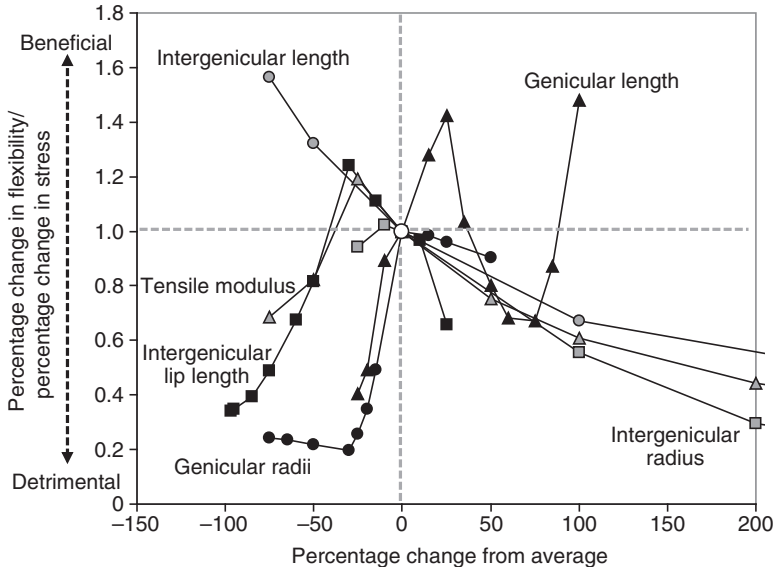

Fig. 7. Effect of varying genicular dimensions on the ratio of flexibility (a presumed benefit) to stress (a presumed cost). Adjustments to genicular dimensions that increased the flexibility:stress ratio were considered net benefits for articulated fronds. Symbols represent changes in genicular radii (black circles), genicular length (black triangles), intergenicular lip length (black squares), intergenicular length (gray circles), tensile modulus (gray triangles) and intergenicular radius (gray squares).

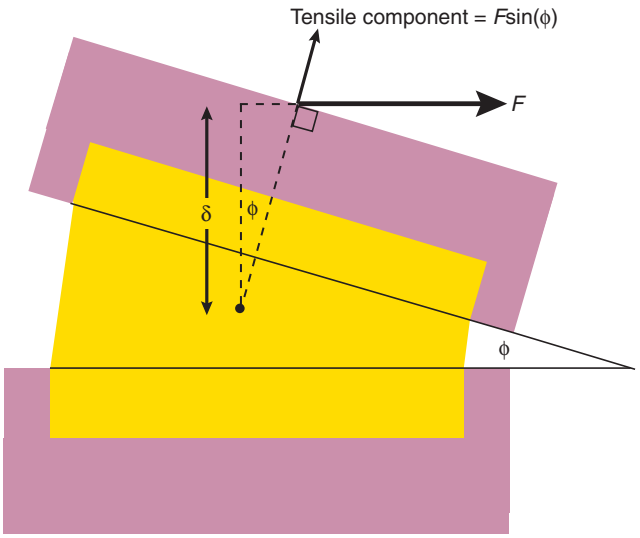

Fig. A1. Diagram of long-sectioned geniculum demonstrating that frond deflections are a consequence of bending angles (ϕ) at each geniculum. Genicular tissue is shown in yellow; intergenicular tissue is shown in pink; δ is the distance from force (*F*) application to the center of the bending geniculum.

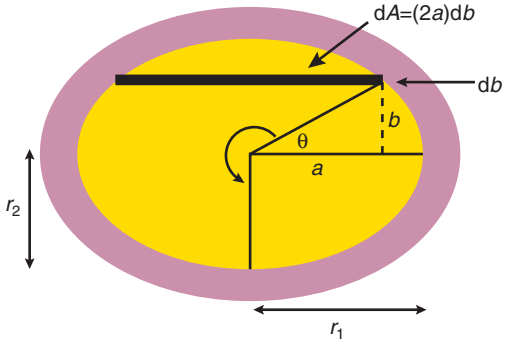

Fig. A2. Diagram of cross-sectioned geniculum indicating how polar coordinates were calculated for each elliptical geniculum. Genicular tissue is shown in yellow; intergenicular tissue is shown in pink; *A* is the unstretched genicular cross-sectional area; r_1 and r_2 are genicular radii; (*a*,*b*) are coordinate positions along the periphery of the elliptical geniculum; and θ is the angle relative to the geniculum center.

with several other algal tissues (Hale, 2001). But genicular tissue can also resist greater stresses than other algal tissues (Martone, 2006). The 'strong and stiff' breakage strategy of genicular tissue can be contrasted with the 'weak and stretchy' strategy of other seaweed tissues (Koehl, 1984; Koehl, 1986; Hale, 2001). Ultimately, the distinct combination of strength and stiffness allows genicula to absorb and resist more than 10 times the energy per volume imposed by breaking waves as that resisted by many other seaweeds (Hale, 2001). Consequently, *Calliarthron* genicula can remain moderately stiff without risking frond breakage.

APPENDIX A
Bending model details

Frond deflections are resisted by the genicula separating each calcified segment (Fig. A1). Fronds reach equilibrium when external and internal moments are equal.

External moments

Given drag force, *F*, applied in the downstream direction perpendicular to an erect frond, we can calculate bending moment, *M*, as:

$$M = F\delta\,, \tag{A1}$$

where δ is the lever arm, the distance from force application to the center of any bending geniculum (Fig. 2A). As fronds bend, lever arms decrease (Fig. 2B). Ultimately, the reduction in lever arm is a function of total bending angle at each geniculum. For example, in Fig. 2:

$$\text{New } \delta_1 = L_1\cos(\phi_1) + L_2\cos(\phi_1 + \phi_2) + L_3\cos(\phi_1 + \phi_2 + \phi_3)\,. \tag{A2}$$

Internal moments

The total internal moment *M* resisted by any geniculum is the sum of elemental moments:

$$M = \int \mathrm{d}M = \int z\mathrm{d}F\,, \tag{A3}$$

where internal moments, like external moments, are the products of forces and lever arms. In this case, elemental moments, d*M*, are the result of elemental forces, d*F*, applied some distance, *z*, away from the neutral axis of the geniculum. The neutral axis is the position within genicular tissue that remains unstressed during bending.

Given the definition of tissue stress σ:

$$\sigma \equiv \frac{F}{A}\,, \tag{A4}$$

it follows that:

$$F = \sigma A\,,$$

$$\mathrm{d}F = \sigma \mathrm{d}A\,, \tag{A5}$$

where *A* is unstretched genicular cross-sectional area, and any elemental force, d*F*, can be expressed as the product of stress and elemental area, d*A* (see Fig. A2). Thus, *M* can be expressed by substituting for *F*:

$$M = \int z\sigma \mathrm{d}A\,. \tag{A6}$$

Given that tissue stiffness *E* is defined as:

$$E \equiv \frac{\sigma}{\varepsilon}$$

$$\sigma = E\varepsilon\,, \tag{A7}$$

where ε is tissue strain, we can substitute for σ to yield:

$$M = \int zE\varepsilon \mathrm{d}A\,. \tag{A8}$$

Using elliptical polar coordinates, we describe positions along the genicular periphery by:

$$a = r_1\cos\theta\,,$$

$$b = r_2\sin\theta\,, \tag{A9}$$

where θ is the angle relative to the geniculum center (Fig. A2). Taking the derivative of the *y*-coordinate:

$$\mathrm{d}b = r_2\cos\theta\mathrm{d}\theta\,. \tag{A10}$$

The area of any elemental rectangular portion of ellipse is:

$$\mathrm{d}A = (2a)\mathrm{d}b$$

$$= 2r_1r_2\cos^2\theta\mathrm{d}\theta\,. \tag{A11}$$

Substituting Eqn A10 into Eqn A8, total internal moment can be expressed as:

$$M = \int_{-\pi/2}^{\pi/2} z\, E\, \varepsilon\, 2 r_1 r_2 \cos^2\theta d\theta \,. \quad \text{(A12)}$$

At this point, we use this equation in two distinct ways to separate the two sequential modes of geniculum bending that occur before and after adjacent intergenicula make contact.

Moments before intergenicula make contact

Before adjacent intergenicula touch, genicula are bent such that all tissue on the upstream side of the neutral axis is stretched *via* tension, while all tissue on the downstream side of the neutral axis is squeezed *via* compression (Fig. A3). By definition, the neutral axis remains unstressed during bending, does not change length, and is located some perpendicular distance, η, away from the genicular midline. The position of the neutral axis depends upon tensile (E_t) and compressive (E_c) moduli, such that moments within tensile and compressive halves are balanced and no net force results. When tensile and compressive moduli are equivalent, the neutral axis passes directly through the center of the tissue. However, tensile and compressive moduli of biological materials are often not equal. Gaylord (Gaylord, 1997) demonstrated that for several kelp tissues:

$$E_t \approx 4E_c \,. \quad \text{(A13)}$$

Here this conclusion is applied to genicular tissue. Tensile moduli are measured experimentally, and then compressive moduli are assumed to be 4 times lower. The result is an off-center neutral axis, shifted toward the tensile side of genicula (Fig. A3).

Using E_t and E_c, we can calculate the exact location of the neutral axis by iteratively solving for η in the following equation, derived in appendix 7 of Gaylord (Gaylord, 1997):

$$\left(E_t - E_c\right)\left(\frac{(r_2^2-\eta^2)^{\frac{3}{2}}}{3} + \frac{\eta r_2^2}{2}\arcsin\left(\frac{\eta}{r_2}\right) + \frac{\eta^2}{2}\sqrt{r_2^2-\eta^2}\right) - \left(E_t + E_c\right)\frac{\eta r_2^2 \pi}{4} = 0 \,. \quad \text{(A14)}$$

Now we can explicitly define the distance, z, between the neutral axis and any elemental area of geniculum (Fig. A3B) over which elemental forces are applied (Eqns A3–A6):

$$z = r_2 \sin\theta - \eta \,. \quad \text{(A15)}$$

Tissue strain, ε, can be calculated from the change in tissue length between intergenicula:

$$\varepsilon_{\text{pre-contact}} = \frac{\omega + 2m}{\omega} - 1 = \frac{2m}{\omega} \,, \quad \text{(A16)}$$

where m is additional length defined by the triangle in Fig. A3A, such that:

$$\sin\left(\frac{\phi}{2}\right) = \frac{m}{r_2 \sin\theta - \eta} \,, \quad \text{(A17)}$$

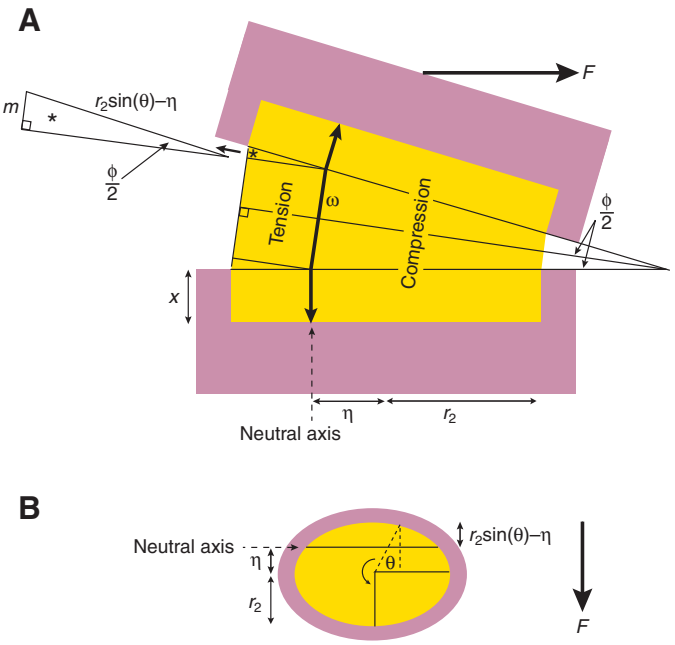

Fig. A3. Diagram of bending geniculum in long-section (A) and cross-section (B) before intergenicula make contact. Genicular tissue is shown in yellow; intergenicular tissue is shown in pink; m is additional length; ω is genicular length; η is the perpendicular distance of the neutral axis from the genicular midline; and x is the intergenicular lip length.

$$m = \left(r_2 \sin\theta - \eta\right)\sin\left(\frac{\phi}{2}\right) \,. \quad \text{(A18)}$$

Note that this model assumes that genicula follow the shortest straight line distance between intergenicula, as if composed of cables, and do not curve like a typical bent solid (see Discussion). Substituting for m in Eqn A16 yields:

$$\varepsilon_{\text{pre-contact}} = \frac{2\left(r_2 \sin\theta - \eta\right)\sin\left(\frac{\phi}{2}\right)}{\omega} \,. \quad \text{(A19)}$$

Then substituting for ε in Eqn A12, we obtain an expression describing the internal moment resisted by genicula bent to angle ϕ before intergenicula make contact:

$$M = \int_{-\pi/2}^{\pi/2}\left(r_2 \sin\theta - \eta\right) E\left(\frac{2\left(r_2 \sin\theta - \eta\right)\sin\left(\frac{\phi}{2}\right)}{\omega}\right) 2 r_1 r_2 \cos^2\theta d\theta \,. \quad \text{(A20)}$$

Intergeniculum contact angle

When intergenicula first make contact, we can define a contact angle ($\phi = 2\beta$), described by a triangle that extends from the point of intergenicular contact to the neutral axis (Fig. A4), such that:

$$\sin\beta = \frac{\left(\frac{\omega - 2x}{2}\right)}{y + \eta} \quad \text{(A21)}$$

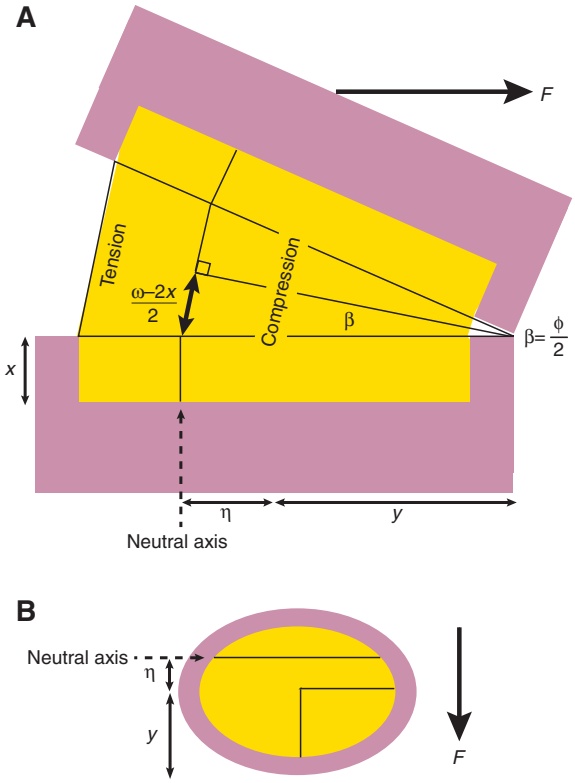

Fig. A4. Diagram of bending geniculum in long-section (A) and cross-section (B) precisely when intergenicula make contact. Genicular tissue is shown in yellow; intergenicular tissue is shown in pink. Contact angle (2β) can be calculated from genicular dimensions.

and $$\beta = \arcsin\left(\frac{\omega - 2x}{2(y+\eta)}\right). \quad \text{(A22)}$$

Moments after intergenicula make contact

When intergenicula touch, the neutral axis – the axis around which a geniculum rotates – abruptly shifts to the point of lip contact and the entire geniculum begins to stretch in tension (Fig. A5). Compressed genicular tissue begins to extend and stretched tissue extends even more.

After contact, the distance away from the neutral axis for any elemental area of geniculum becomes the sum of the intergenicular radius y and the polar coordinate b:

$$z = y + b = y + r_2\sin\theta\,. \quad \text{(A23)}$$

Again, tissue strain (ε) can be calculated as the change in length of genicular tissue between intergenicula (see Fig. A5):

$$\varepsilon_{\text{post-contact}} = \frac{2k + 2x}{\omega} - 1\,, \quad \text{(A24)}$$

where k is half the new length of genicular tissue defined by the triangle depicted in Fig. A5, such that:

$$\sin\left(\frac{\phi}{2}\right) = \frac{k}{y + r_2\sin\theta}\,, \quad \text{(A25)}$$

$$k = \left(y + r_2\sin\theta\right)\sin\left(\frac{\phi}{2}\right). \quad \text{(A26)}$$

Substituting for k in Eqn A24 yields:

$$\varepsilon_{\text{post-contact}} = \frac{2\left(y + r_2\sin\theta\right)\sin\left(\frac{\phi}{2}\right) + 2x}{\omega} - 1\,. \quad \text{(A27)}$$

To account for tissue strain before intergenicula made contact ($\phi \le 2\beta$), we combine Eqns A19 and A27 as follows:

$$\begin{aligned}\varepsilon_{\text{total}} &= \varepsilon_{\text{pre-contact}} + \varepsilon_{\text{post-contact}} \\ &= \frac{2\left(r_2\sin\theta - \eta\right)\sin\left(\beta\right)}{\omega} + \frac{2\left(y + r_2\sin\theta\right)\sin\left(\frac{\phi}{2} - \beta\right) + 2x}{\omega} - 1 \\ &= \frac{2\left(r_2\sin\theta - \eta\right)\sin\left(\beta\right) + 2\left(y + r_2\sin\theta\right)\sin\left(\frac{\phi}{2} - \beta\right) + 2x}{\omega} - 1\,.\end{aligned} \quad \text{(A28)}$$

Finally substitution for ε in Eqn A12 yields an expression describing the internal moment resisted by genicula bent to angle ϕ after intergenicula made contact:

$$M = \int_{-\pi/2}^{\pi/2}\left(y + r_2\sin\theta\right)E \left(\frac{2\left(r_2\sin\theta - \eta\right)\sin\left(\beta\right) + 2\left(y + r_2\sin\theta\right)\sin\left(\frac{\phi}{2} - \beta\right) + 2x}{\omega} - 1\right) 2r_1 r_2\cos^2\theta\, d\theta\,. \quad \text{(A29)}$$

Implementation of geometry in Matlab

The above geometrical relationships were incorporated into a Matlab routine in order to predict the deflection of articulated fronds by applied forces. In practice, genicular dimensions for 10 genicula and an applied force were inserted into the model. Bending angles (2β) at which intergenicula make contact were calculated. Moments required to bend genicula before and after intergenicula make contact were calculated by iteratively solving Eqns A20 and A29, respectively, for three arbitrary values of ϕ (0.4, 0.8, 1.0), using E=E_c for negative strains and E=E_t for positive strains. Linear regressions were fitted to the two sets of three (M,ϕ) datapoints and were subsequently used to quickly calculate ϕ for genicula given applied moments.

The model initially applied a small fraction (1/100) of the total force at the frond apex and calculated external moments at all genicula (Eqns A1 and A2; Fig. 2). Moments were used to calculate bending angles at all genicula, using the linear regression described above, assuming intergenicula had not yet made contact. Lever arms were re-calculated, given the bending angles (Eqn A2), force was incremented, and external moments were re-calculated at all genicula (Eqns A1 and A2). Moments were used to calculate new bending angles, using 'after contact' linear regressions if previous angles exceeded 2β. Bending angles and incremented force were used to re-calculate lever arms and external moments, and new angles were calculated using moment regressions. This process was repeated until maximum force was applied.

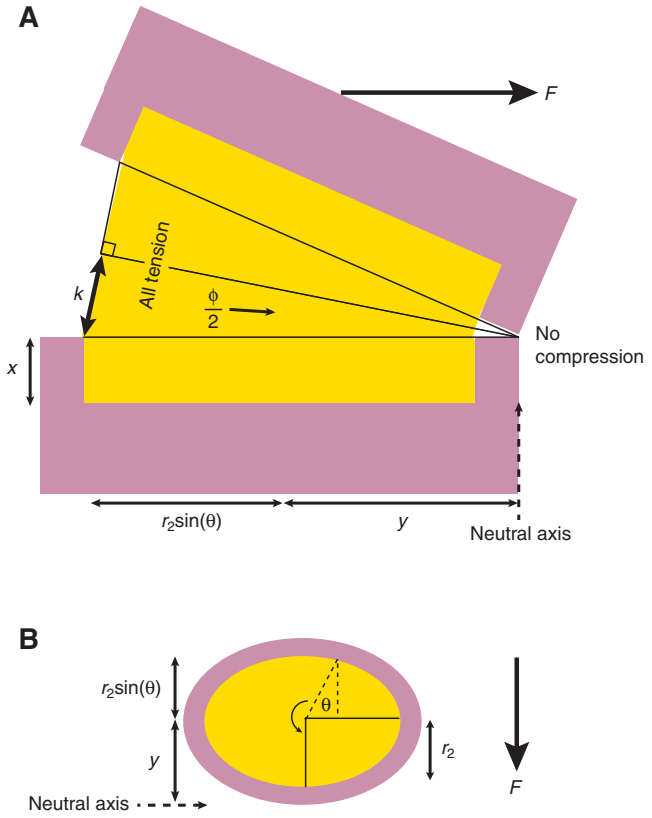

Fig. A5. Diagram of bending geniculum in long-section (A) and cross-section (B) after intergenicula make contact. Genicular tissue is shown in yellow; intergenicular tissue is shown in pink; *k* is half the new length of genicular tissue.

APPENDIX B
Maximum stress in first geniculum

The model computed maximum stress (i.e. stress in the outermost tissue, $\theta=\pi/2$) in the first geniculum bent to ϕ_1. Total stress was calculated as the sum of stresses caused by bending and tensile components. Bending stresses were calculated from strains resulting from geniculum bending angles (Eqns A19 and A28), and tensile stresses were calculated as tensile force per cross-sectional area of elliptical geniculum (Fig. A1):

$$\sigma_{\text{total}} = \sigma_{\text{bending}} + \sigma_{\text{tension}} = E_t\varepsilon + \frac{F\sin(\phi_1)}{\pi r_1 r_2}. \quad \text{(A30)}$$

Tensile stresses were generally one to two orders of magnitude less than bending stresses in this study, but become increasingly important as fronds bend to 90 deg. Note that once fronds reach 90 deg., bending stresses are maximized but tensile stresses continue to increase with increasing force.

For $\phi_1 \leq 2\beta$, Eqn A30 was solved using strain before intergenicula make contact (Eqn A19):

$$\sigma_{\max} = E_t\left(\frac{2(r_2-\eta)\sin\left(\frac{\phi_1}{2}\right)}{\omega}\right) + \frac{F\sin(\phi_1)}{\pi r_1 r_2}. \quad \text{(A31)}$$

For $\phi_1 > 2\beta$, Eqn A30 was solved using strain after intergenicula make contact (Eqn A28):

$$\sigma_{\max} = E_t\left(\frac{2(r_2-\eta)\sin(\beta)+2(y+r_2)\sin\left(\frac{\phi_1}{2}-\beta\right)+2x}{\omega}-1\right)+\frac{F\sin(\phi_1)}{\pi r_1 r_2}. \quad \text{(A32)}$$

Because of the subtle interactions between genicular dimensions, bending angle (ϕ_1) and intergeniculum contact angle (β), varying any one dimension can have non-linear, cyclical effects on stress (Eqns A31 and A32), as described below.

Genicular length

Slight increases in ω decrease stress, but as ω continues to increase, ϕ_1 increases rapidly as fronds bend over, causing tissue stress to increase (Fig. 6A). Once fronds bend 90 deg. (the maximum bending angle, ϕ_1), additional increases in ω increase β and drive tissue stress down.

Genicular radius

Increasing r_1 and r_2 causes a slight decrease in ϕ_1, a slight increase in other terms (Eqn A32) and, ultimately, has very little effect on stress. Decreasing r_1 and r_2 causes ϕ_1 to increase rapidly, increasing tissue stress (Fig. 6B). Once fronds bend to 90 deg., further reduction in r_2 causes stress to decline.

Intergenicular lip length

Decreasing x initially has little effect on ϕ_1, but causes stress to decrease. Further decreases in x cause ϕ_1 to increase rapidly, increasing stress.

Tensile modulus

Decreasing E_t initially causes tissue stress to decrease, but eventually causes ϕ_1 to increase, driving stress back up.

This manuscript benefited from comments made by M. Boller, K. Mach, L. Miller, K. Miklasz, R. Martone and two anonymous reviewers. Research was supported by the Phycological Society of America, the Earl and Ethyl Myers Oceanographic and Marine Biology Trust, and NSF Grant no. IOS-0641068 to M.W.D. This is contribution number 308 from PISCO, the Partnership for Interdisciplinary Studies of Coastal Oceans, funded primarily by the Gordon and Betty Moore Foundation and the David and Lucile Packard Foundation.

REFERENCES

Bell, E. C. (1999). Applying flow tank measurements to the surf zone: predicting dislodgment of the Gigartinaceae. *Phycol. Res.* **47**, 159-166.
Bell, E. C. and Denny, M. W. (1994). Quantifying 'wave exposure': a simple device for recording maximum velocity and results of its use at several field sites. *J. Exp. Mar. Biol. Ecol.* **181**, 9-29.
Blanchette, C. A. (1997). Size and survival of intertidal plants in response to wave action: a case study with *Fucus gardneri*. *Ecology* **78**, 1563-1578.
Boller, M. L. and Carrington, E. (2006). The hydrodynamic effects of shape and size change during reconfiguration of a flexible macroalga. *J. Exp. Biol.* **209**, 1894-1903.
Carrington, E. (1990). Drag and dislodgement of an intertidal macroalga: consequences of morphological variation in *Mastocarpus papillatus* Kutzing. *J. Exp. Mar. Biol. Ecol.* **139**, 185-200.
Delf, E. M. (1932). Experiments with the stipes of *Fucus* and *Laminaria*. *J. Exp. Biol.* **9**, 300-313.
Denny, M. W. (1988). *Biology and Mechanics of The Wave-Swept Environment.* Princeton, NJ: Princeton University Press.
Denny, M. W. (1995). Predicting physical disturbance: mechanistic approaches to the study of survivorship on wave-swept shores. *Ecol. Monogr.* **65**, 371-418.

Denny, M. W. and Gaylord, B. (2002). The mechanics of wave-swept algae. *J. Exp. Biol.* **205**, 1355-1362.
Denny, M. W., Miller, L. P., Stokes, M. D., Hunt, L. J. H. and Helmuth, B. S. T. (2003). Extreme water velocities: topographical amplification of wave-induced flow in the surf zone of rocky shores. *Limnol. Oceanogr.* **48**, 1-8.
Dudgeon, S. R. and Johnson, A. S. (1992). Thick vs. thin: thallus morphology and tissue mechanics influence differential drag and dislodgement of two co-dominant seaweeds. *J. Exp. Mar. Biol. Ecol.* **165**, 23-43.
Etnier, S. A. (2001). Flexural and torsional stiffness in multi-jointed biological beams. *Biol. Bull.* **200**, 1-8.
Etnier, S. A. (2003). Twisting and bending of biological beams: distribution of biological beams in a stiff mechanospace. *Biol. Bull.* **205**, 35-46.
Friedland, M. T. and Denny, M. W. (1995). Surviving hydrodynamic forces in a wave-swept environment: consequences of morphology in the feather boa kelp, *Egregia menziesii* (Turner). *J. Exp. Mar. Biol. Ecol.* **190**, 109-133.
Gaylord, B. (1997). Consequences of wave-induced water motion to nearshore macroalgae. PhD Thesis, Stanford University, Stanford, CA.
Gaylord, B. and Denny, M. W. (1997). Flow and flexibility. I. effects of size, shape and stiffness in determining wave forces on the stipitate kelps *Eisenia arborea* and *Pterygophora californica*. *J. Exp. Biol.* **200**, 3141-3164.
Hale, B. (2001). Macroalgal materials: foiling fracture and fatigue from fluid forces. PhD Thesis, Stanford University, Stanford, CA.
Harder, D., Speck, O., Hurd, C. and Speck, T. (2004). Reconfiguration as a prerequisite for survival in highly unstable flow-dominated environments. *J. Plant Growth Regul.* **23**, 98-107.
Harder, D., Hurd, C. and Speck, T. (2006). Comparison of mechanical properties of four large, wave-exposed seaweeds. *Am. J. Bot.* **93**, 1426-1432.
Johansen, H. W. (1969). Morphology and systematics of coralline algae with special reference to *Calliarthron*. *Univ. Calif. Publ. Bot.* **49**, 1-98.
Johansen, H. W. (1981). *Coralline Algae, A First Synthesis*. Boca Raton: CRC Press.
Johnson, J. H. (1961). *Limestone-Building Algae and Algal Limestones*. Boulder: Colorado School of Mines.
Koehl, M. A. R. (1977). Mechanical organization of cantilever-like sessile organisms: sea anemones. *J. Exp. Biol.* **69**, 127-142.
Koehl, M. A. R. (1984). How do benthic organisms withstand moving water? *Am. Zool.* **24**, 57-70.
Koehl, M. A. R. (1986). Seaweeds in moving water: form and mechanical function. In *On the Economy of Plant Form and Function* (ed. T. J. Givnish), pp. 603-634. Cambridge: Cambridge University Press.
Martone, P. T. (2006). Size, strength and allometry of joints in the articulated coralline *Calliarthron*. *J. Exp. Biol.* **209**, 1678-1689.
Martone, P. T. (2007). Kelp versus coralline: cellular basis for mechanical strength in the wave-swept seaweed *Calliarthron* (Corallinaceae, Rhodophyta). *J. Phycol.* **43**, 882-891.
Martone, P. T. and Denny, M. W. (2008). To break a coralline: mechanical constraints on the size and survival of a wave-swept seaweed. *J. Exp. Biol.* **211**, 3433-3441.
Niklas, K. J. (1992). *Plant Biomechanics: An Engineering Approach to Plant Form and Function*. Chicago: University of Chicago Press.
O'Donnell, M. (2005). Habitats and hydrodynamics on wave-swept rocky shores. PhD Thesis, Stanford University, Stanford, CA.
Padilla, D. K. (1993). Rip stop in marine algae: minimizing the consequences of herbivore damage. *Evol. Ecol.* **7**, 634-644.
Steneck, R. S. (1983). Escalating herbivory and resulting adaptive trends in calcareous algal crusts. *Paleobiology* **9**, 44-61.
Steneck, R. S. (1986). The ecology of coralline algal crusts: convergent patterns and adaptive strategies. *Ann. Rev. Ecol. Syst.* **17**, 273-303.
Vogel, S. (1984). Drag and flexibility in sessile organisms. *Am. Zool.* **24**, 37-44.
Wainwright, S. A., Biggs, W. D., Currey, J. D. and Gosline, J. M. (1982). *Mechanical Design in Organisms*. Princeton, NJ: Princeton University Press.
Wray, J. L. (1977). *Calcareous Algae*. New York: Elsevier.